

Nonreciprocal photon blockade via quadratic optomechanical coupling

Xun-Wei Xu,^{1,*} Yan-Jun Zhao,^{2,3} Hui Wang,⁴ Hui Jing,⁵ and Ai-Xi Chen^{6,1,†}

¹*Department of Applied Physics, East China Jiaotong University, Nanchang, 330013, China*

²*Beijing National Laboratory for Condensed Matter Physics,*

Institute of Physics, Chinese Academy of Sciences, Beijing 100190, China

³*School of Physical Sciences, University of Chinese Academy of Sciences, Beijing 100190, China*

⁴*Advanced Device Laboratory, RIKEN, Wako, Saitama 351-0198, Japan*

⁵*Key Laboratory of Low-Dimensional Quantum Structures and Quantum Control of Ministry of Education, Department of Physics and Synergetic Innovation Center for Quantum Effects and Applications, Hunan Normal University, Changsha 410081, China*

⁶*Department of Physics, Zhejiang Sci-Tech University, Hangzhou 310018, China*

(Dated: September 21, 2018)

We propose to manipulate the statistic properties of the photons transport nonreciprocally via quadratic optomechanical coupling. We present a scheme to generate quadratic optomechanical interactions in the normal optical modes of a whispering-gallery-mode (WGM) optomechanical system by eliminating the linear optomechanical couplings via anticrossing of different modes. By optically pumping the WGM optomechanical system in one direction, the effective quadratic optomechanical coupling in that direction will be enhanced significantly, and nonreciprocal photon blockade will be observed consequently. Our proposal has potential applications for the on-chip nonreciprocal single-photon devices.

I. INTRODUCTION

Nonreciprocal devices [1], such as isolators and circulators, have drawn an immense amount of interest in the past few years, for their irreplaceable role in signal processing and communication. One of the key parameters for nonreciprocal devices is the isolation, and almost all the studies on nonreciprocity focus on the transmission properties of the nonreciprocal devices. However, whether the statistic properties of the transmitted photons have been changed and how to manipulate the statistic properties of the transmitted photons in nonreciprocal devices are rarely discussed.

Recently, the statistic properties of the transmitted photons in rotating nonlinear devices were discussed theoretically [2], and a quantum effect called nonreciprocal photon blockade was predicted, that photon blockade can emerge when the resonator is driven in one direction but not the other. Physically, the nonreciprocal photon blockade is induced by the Fizeau-Sagnac drag [3–5], which leads to a split of the resonance frequencies of the counter-circulating modes. Similarly, nonreciprocal transport [6, 7] and localization [8] of photons have been demonstrated based on the Doppler shift in moving photonic lattice made. In contrast to the classical nonreciprocal behaviors, purely quantum effects in nonreciprocal devices were proposed in reference [2], which opens up the prospect of exploring nonreciprocal quantum effects, such as nonreciprocal single-photon blockades, nonreciprocal two-photon blockades, and nonreciprocal photon-induced tunneling.

An optomechanical system, that resonance frequency of a cavity mode depends on the position a mechanical mode via radiation pressure or optical gradient forces, provides us an appropriate platform to manipulate photons (for reviews, see Refs. [9–14]). Lately, several theoretical [15–25] and experimental [26–36] works have demonstrated that optomechanical interaction can lead to nonreciprocal transport of photons. One of the proposals for nonreciprocity is based on the inherent nontrivial topology in whispering-gallery-mode (WGM) optomechanical system [16], where the effective optomechanical coupling is enhanced in one direction and suppressed in the other one by optically pumping the ring resonator. But the enhanced effective optomechanical coupling is a simple bilinear interaction, which can not be used to manipulate the statistic properties of the nonreciprocal transport photons. Fortunately, Xie *et al.* proposed to generate strong quadratic (nonlinear) optomechanical coupling by a strong driving optical field, and the appearance of strong photon antibunching was predicted in a quadratically coupled optomechanical system under single-photon weak coupling conditions [37].

Motivated by the pioneering work on nonreciprocal quantum effects [2], we propose to manipulate the statistic properties of the nonreciprocal transport photons in a WGM optomechanical system [16] with quadratic optomechanical interactions [37]. Employing a similar idea given in Refs. [38–41], quadratic optomechanical interactions can be generated in the normal optical modes of a WGM optomechanical system by eliminating the linear optomechanical couplings via anticrossing of different modes. We demonstrate that quadratic optomechanical interactions can not only induce nonreciprocal photon transport, but also manipulate the statistic properties of the nonreciprocal transport photons. For example, photon blockade with high transmission coefficient

* davidxu0816@163.com

† aixichen@ecjtu.edu.cn

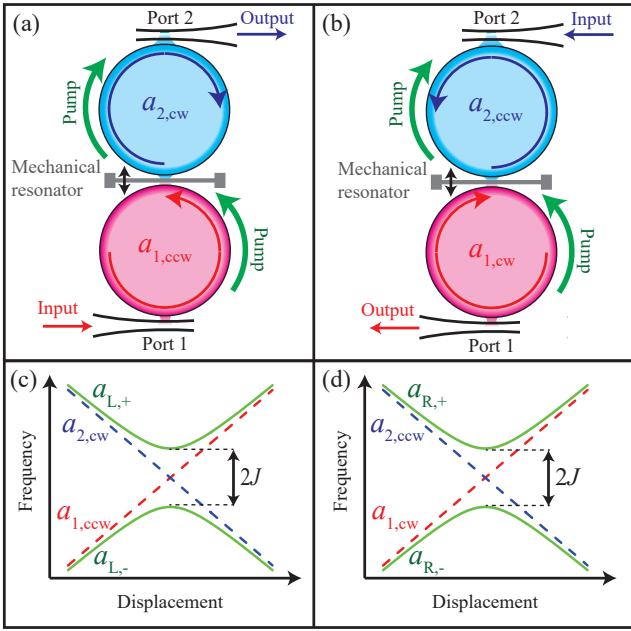


FIG. 1. (Color online) (a) and (b) Schematic diagram for generating quadratic optomechanical coupling, where a mechanical nanostring oscillator is placed between two whispering gallery mode (WGM) resonators. (c) and (d) Dispersion of the optical modes as a function of the displacement.

can be observed when the photons transport in one direction but not the other. WGM optomechanical systems with quadratic optomechanical interactions can be used to design nonreciprocal single-photon devices in integrated photonic chips.

The remainder of this paper is organized as follows. In Sec. II, we propose an system consisting of two whispering gallery mode (WGM) resonators quadratically coupling with a common mechanical mode. In Sec. III, the effective Hamiltonian of an optomechanical system with quadratic coupling is obtained with one optical mode driven by a strong external field. In Sec. IV, we show that the optomechanical system with quadratic coupling can be used to realize nonreciprocal photon blockade. Finally, the main results are summarized in Sec. V.

II. QUADRATIC OPTOMECHANICAL COUPLING

One of the most major ingredients in optomechanical system is that the resonance frequency of a cavity mode is dependent on the position of a mechanical mode. It is well known that the cavity frequency of a WGM optomechanical system is almost linearly proportional to the the mechanical position [42], even though the effects of quadratic optomechanical coupling have also been observed in experiments [43, 44]. In this section we will show how to generate a quadratic optomechanical coupling as the dominant coupling in the situation when the

linear optomechanical coupling vanishes.

As shown in Fig. 1(a) and 1(b), the setup we consider here consists of one mechanical resonator optomechanical coupling to two optical resonators ($j = 1, 2$) via the optical evanescent field, with each optical resonator supporting two degenerate clockwise (CW) and counter-clockwise (CCW) travelling-wave whispering-gallery modes (WGMs). This model can be described by the optomechanical interaction Hamiltonian

$$H_{\text{om}} = \sum_{j=1,2} \sum_{\lambda=\text{cw,ccw}} \left[\omega_0 + (-1)^j g_0 q \right] a_{j,\lambda}^\dagger a_{j,\lambda} + J \left(a_{1,\text{ccw}} a_{2,\text{cw}}^\dagger + a_{1,\text{cw}} a_{2,\text{ccw}}^\dagger + \text{H.c.} \right) + \frac{1}{2} \omega_m (q^2 + p^2), \quad (1)$$

where $a_{j,\lambda}$ and $a_{j,\lambda}^\dagger$ ($j = 1, 2$ and $\lambda = \text{cw, ccw}$) are the annihilation and creation operators of the optical modes with frequency ω_0 ; J is the tunneling amplitude between the optical modes; q and p are the dimensionless displacement and momentum operators of the mechanical resonator with frequency ω_m , and g_0 is the linear optomechanical coupling strength between the mechanical resonator and optical modes. We assume that the optical mode $a_{j,\lambda}$ is coupled to a waveguide (Port j) with strength γ_c , and the damping rate of mechanical resonator q is γ_m .

Following the approach in Refs. [38–41], where $|J| \gg \omega_m$ is assumed such that q can be treated as a quasi-static variable, the Hamiltonian can be diagonalized as

$$H_{\text{om}} = \sum_{j=L,R} \sum_{\lambda=\pm} \omega_\lambda(q) a_{j,\lambda}^\dagger a_{j,\lambda} + \frac{1}{2} \omega_m (q^2 + p^2), \quad (2)$$

in the normal modes basis, $a_{L,\pm} = [J a_{1,\text{ccw}} + (g_0 q \pm \sqrt{J^2 + (g_0 q)^2}) a_{2,\text{cw}}] / D_\pm$ and $a_{R,\pm} = [J a_{1,\text{cw}} + (g_0 q \pm \sqrt{J^2 + (g_0 q)^2}) a_{2,\text{ccw}}] / D_\pm$, with $D_\pm^2 = J^2 + (g_0 q \pm \sqrt{J^2 + (g_0 q)^2})^2$, and eigenfrequencies

$$\omega_\pm(q) = \omega_0 \pm \sqrt{J^2 + (g_0 q)^2} \quad (3)$$

as shown in Figs. 1(c) and 1(d). Moreover, $|J| \gg g_0 q$ is assumed such that we can Taylor expand the eigenfrequencies as

$$\omega_\pm(q) \approx \omega_\pm \pm \frac{g_0^2}{2J} q^2 \quad (4)$$

with frequencies $\omega_\pm \equiv \omega_\pm(0) = \omega_0 \pm J$, and the quasi-static Hamiltonian, with quadratic optomechanical coupling $g \equiv g_0^2 / (2J)$ between the mechanical resonator and quasi-static normal optical modes, $a_{L,\pm} \approx (a_{1,\text{ccw}} \pm a_{2,\text{cw}}) / \sqrt{2}$ and $a_{R,\pm} \approx (a_{1,\text{cw}} \pm a_{2,\text{ccw}}) / \sqrt{2}$, is given approximately by

$$H_{\text{om}} \approx (\omega_+ + g q^2) \left(a_{L,+}^\dagger a_{L,+} + a_{R,+}^\dagger a_{R,+} \right) + (\omega_- - g q^2) \left(a_{L,-}^\dagger a_{L,-} + a_{R,-}^\dagger a_{R,-} \right) + \frac{1}{2} \omega_m (q^2 + p^2). \quad (5)$$

As already shown in the experiment [41], when the tunneling amplitude between the optical modes J is larger than the optical damping rates γ_c , the transmission spectrum of a laser probe through the coupled optical modes features resonance dips at the normal resonance frequencies ω_{\pm} , not at the bare optical resonance frequencies ω_0 . That is to say, the normal modes are coupled to the external waveguides and can be used to describe the input-output characteristic of the coupled optical modes system. Specifically, the total loss damping rate of the normal modes $a_{L/R,\pm}$ is γ_c for $a_{R,\pm} \approx [a_{1,cw} \pm a_{2,ccw}]/\sqrt{2}$, and they are coupled to both the two ports with strength $\gamma_c/2$, respectively.

III. DIRECTIONAL NONLINEAR INTERACTION

In this section, we choose either pair of degenerated quasi-static normal optical modes ($a_{L,+}$ and $a_{R,+}$, or $a_{L,-}$ and $a_{R,-}$), to generate strong nonlinear interaction for few photons traveling in one direction, but not in the reverse direction. Without loss of generality, the two optical modes are denoted as a_L and a_R , with frequency $\omega_a = \omega_+ \text{ or } \omega_-$, for photons travelling from port 1 to port 2 and the opposite direction, respectively. To enhance the nonlinear optomechanical coupling between the optical mode a_L and the mechanical resonator, the optical mode a_L is pumped by a strong field with amplitude $\Omega \gg \gamma_c$ and frequency $\omega_L \sim \omega_a - 2\omega_m$. In the rotating reference frame with the optical frequency ω_L , the system can be described by a Hamiltonian as

$$H = (\Delta_a + gq^2) (a_L^\dagger a_L + a_R^\dagger a_R) + \frac{1}{2}\omega_m (q^2 + p^2) + \Omega a_L^\dagger + \Omega a_L, \quad (6)$$

with detuning $\Delta_a = \omega_a - \omega_d$.

Under strong driving condition, we perform the displacement transformations: $a_L \rightarrow \alpha_L + a_L$, $a_R \rightarrow \alpha_R + a_R$, $q \rightarrow q_s + q$ and $p \rightarrow p_s + p$, where α_L , α_R , q_s and p_s are the steady state values, and a_L , a_R , q , and p (on the right side of the arrow) are the quantum fluctuation operators. The steady state values α_L , α_R , q_s and p_s can be obtained by the equations of motions yielding $\alpha_L = -i2\Omega/(\gamma_c + i2\Delta_a)$, and $\alpha_R = q_s = p_s = 0$. The operators q and p for the mechanical resonator can be written in terms of phonon creation and annihilation operators as $q = (b^\dagger + b)/\sqrt{2}$, $p = i(b^\dagger - b)/\sqrt{2}$, and the effective Hamiltonian for the quantum fluctuation operators reads

$$H_{\text{eff}} = \Delta_a a_L^\dagger a_L + \Delta_a a_R^\dagger a_R + \omega_m b^\dagger b + \frac{g}{2} (|\alpha|^2 + a_L^\dagger a_L + a_R^\dagger a_R) (b^\dagger + b)^2 + \frac{g}{2} (\alpha_L a^\dagger + \alpha^* a) (b^\dagger + b)^2. \quad (7)$$

We assume that the optical driving field is strong enough so the steady state value α_L is much larger than the quantum fluctuation operators a , i.e., $|\alpha_L|^2 \gg \langle a_L^\dagger a_L \rangle \sim \langle a_R^\dagger a_R \rangle$, and the term $g(a_L^\dagger a_L + a_R^\dagger a_R)(b^\dagger + b)^2$ in the above equation can be neglected safely. For $\Delta_a \sim 2\omega_m \gg |g\alpha_L|/2$, the effective Hamiltonian can be further simplified by rotating-wave approximation and neglecting the high frequency terms b^2 and ab^2 yielding

$$H_{\text{eff}} = \Delta_a (a_L^\dagger a_L + a_R^\dagger a_R) + \omega'_m b^\dagger b + G a_L^\dagger b^2 + G^* a_L b^{\dagger 2}, \quad (8)$$

where $\omega'_m = \omega_m + g|\alpha|^2$ is the effective mechanical frequency, and $G = g\alpha_L/2$ is the effective nonlinear coupling strength between the optical and mechanical modes. Without loss of generality G is assumed to be real in the following.

To investigate the system's response behavior to weak prob fields, a weak field with amplitude $\varepsilon \ll \gamma_c$ and frequency $\omega_p \approx \omega_a$ is input from one of the ports. The total Hamiltonian is given by

$$H_{\text{tot}} = H_{\text{eff}} + H_{\text{probe}}, \quad (9)$$

where H_{probe} describes the probe field. If the probe field is input from port 1, it can be described by

$$H_{\text{probe}} = \varepsilon e^{-i\delta t} a_L^\dagger + \text{H.c.}, \quad (10)$$

while if the weak field is input from port 2, it can be given by

$$H_{\text{probe}} = \varepsilon e^{-i\delta t} a_R^\dagger + \text{H.c.}, \quad (11)$$

where $\delta = \omega_p - \omega_d$ is the detuning between the strong driving and weak probe fields. In the rotating reference frame with the unitary operator $R'(t) = \exp[i\delta(a_L^\dagger a_L + a_R^\dagger a_R + b^\dagger b/2)t]$, H_{probe} becomes time independent, and the effective Hamiltonian becomes

$$H_{\text{eff}} = \Delta a_L^\dagger a_L + \Delta a_R^\dagger a_R + \Delta_m b^\dagger b + G a_L^\dagger b^2 + G^* a_L b^{\dagger 2}, \quad (12)$$

where the detunings $\Delta = \Delta_a - \delta$ and $\Delta_m = \omega_m + g|\alpha|^2 - \delta/2$ satisfy the condition $\max\{|\Delta|, |\Delta_m|\} \ll \omega_m$.

According to the input-output relations [45], we have $a_{1,\text{in}} = \varepsilon/\sqrt{\gamma_c/2}$ and $a_{2,\text{out}} = \sqrt{\gamma_c/2}a_L$ ($a_{2,\text{in}} = \varepsilon/\sqrt{\gamma_c/2}$ and $a_{1,\text{out}} = \sqrt{\gamma_c/2}a_R$), and then the transmission coefficient for the weak probe field can be defined by

$$T_{21} \equiv \frac{\langle a_{2,\text{out}}^\dagger a_{2,\text{out}} \rangle}{\langle a_{1,\text{out}}^\dagger a_{1,\text{out}} \rangle} = \frac{\gamma_c^2}{4\varepsilon} \langle a_L^\dagger a_L \rangle \quad (13)$$

for photon transport from port 1 to port 2, and

$$T_{12} \equiv \frac{\langle a_{1,\text{out}}^\dagger a_{1,\text{out}} \rangle}{\langle a_{2,\text{out}}^\dagger a_{2,\text{out}} \rangle} = \frac{\gamma_c^2}{4\varepsilon} \langle a_R^\dagger a_R \rangle \quad (14)$$

for photon transport from port 2 to port 1, where $n_L \equiv \langle a_L^\dagger a_L \rangle$ and $n_R \equiv \langle a_R^\dagger a_R \rangle$ are the mean photon numbers. The isolation for probe field transport from port 1 to port 2 is defined by

$$I \equiv \frac{T_{12}}{T_{21}}. \quad (15)$$

Using the input-output relations: $a_{1,\text{in}} = \varepsilon/\sqrt{\gamma_c/2}$ and $a_{2,\text{out}} = \sqrt{\gamma_c/2}a_L$ ($a_{2,\text{in}} = \varepsilon/\sqrt{\gamma_c/2}$ and $a_{1,\text{out}} = \sqrt{\gamma_c/2}a_R$), the statistic properties of the transmitted photons $a_{2,\text{out}}$ and $a_{1,\text{out}}$ can be described by the second-order correlation functions in the steady state ($t \rightarrow \infty$)

$$\begin{aligned} g_{21}^{(2)}(\tau) &\equiv \frac{\langle a_{2,\text{out}}^\dagger(t) a_{2,\text{out}}^\dagger(t+\tau) a_{2,\text{out}}(t+\tau) a_{2,\text{out}}(t) \rangle}{\langle a_{2,\text{out}}^\dagger(t) a_{2,\text{out}}(t) \rangle^2} \\ &= \frac{\langle a_L^\dagger(t) a_L^\dagger(t+\tau) a_L(t+\tau) a_L(t) \rangle}{\langle a_L^\dagger(t) a_L(t) \rangle^2} \end{aligned} \quad (16)$$

for photon transport from port 1 to port 2, and

$$\begin{aligned} g_{12}^{(2)}(\tau) &\equiv \frac{\langle a_{1,\text{out}}^\dagger(t) a_{1,\text{out}}^\dagger(t+\tau) a_{1,\text{out}}(t+\tau) a_{1,\text{out}}(t) \rangle}{\langle a_{1,\text{out}}^\dagger(t) a_{1,\text{out}}(t) \rangle^2} \\ &= \frac{\langle a_R^\dagger(t) a_R^\dagger(t+\tau) a_R(t+\tau) a_R(t) \rangle}{\langle a_R^\dagger(t) a_R(t) \rangle^2} \end{aligned} \quad (17)$$

for photon transport from port 2 to port 1.

In the next section, the transmission coefficients and correlation functions will be obtained by numerically solving the master equation for the density matrix ρ of the system [46]

$$\begin{aligned} \frac{\partial \rho}{\partial t} &= -i[H_{\text{tot}}, \rho] + \gamma_c L[a_L]\rho + \gamma_c L[a_R]\rho \\ &\quad + \gamma_m (n_{\text{th}} + 1) L[b]\rho + \gamma_m n_{\text{th}} L[b^\dagger]\rho, \end{aligned} \quad (18)$$

where $L[o]\rho = o\rho o^\dagger - (o^\dagger o \rho + \rho o^\dagger o)/2$ denotes a Lindblad term for an operator o ; n_{th} is the mean thermal phonon number, given by the Bose-Einstein statistics $n_{\text{th}} = [\exp(\hbar\omega_m/k_B T) - 1]^{-1}$ with the Boltzmann constant k_B and the temperature T of the reservoir at the thermal equilibrium.

IV. NONRECIPROCAL PHOTON BLOCKADE

In Fig. 2(a), we show the transmission coefficients T_{21} for probe field transport from port 1 to port 2, and T_{12} for probe field transport from port 2 to port 1. For T_{21} , there are two peaks at $\Delta = \pm\sqrt{2}G$ and one dip at $\Delta = 0$. In contrast, there is only one peak at $\Delta = 0$ for T_{12} . Figure 2(b) shows the isolation $I = T_{21}/T_{12}$ for probe field transport from port 1 to port 2 as a function of the

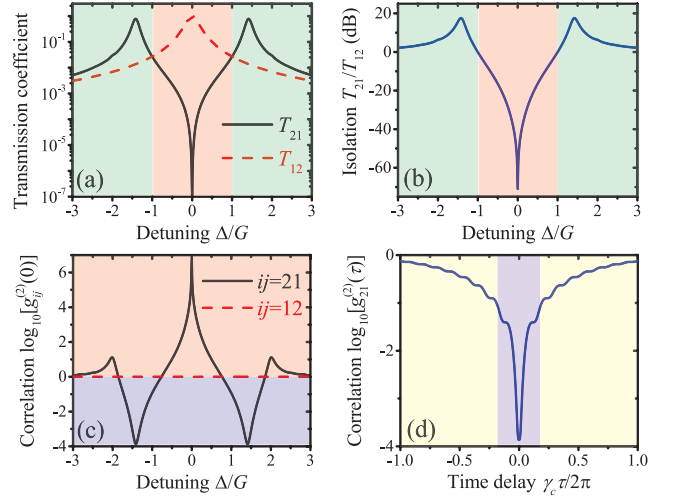


FIG. 2. (Color online) (a) The transmission coefficients T_{21} (solid black curve) and T_{12} (dashed red curve) as a function of the detuning Δ/G . (b) The isolation as a function of the detuning Δ/G . (c) The equal-time second-order correlation function $\log_{10}[g_{ij}^{(2)}(0)]$ ($ij = 12, 21$) as a function of the detuning Δ/G . (d) The second-order correlation function $\log_{10}[g_{21}^{(2)}(\tau)]$ as a function of the normalized time delay $\gamma_c \tau / 2\pi$ at detuning $\Delta = \sqrt{2}G$. The other parameters are $\Delta_m = \Delta/2$, $G = 3\gamma_c$, $\varepsilon = \gamma_c/10$, $\gamma_m = \gamma_c/100$, and $n_{\text{th}} = 0$.

detuning Δ/G . Isolation for the direction $1 \rightarrow 2$ is more than 17 dB at detuning $\Delta = \pm\sqrt{2}G$, and isolation for the reverse direction of $2 \rightarrow 1$ is more than 70 dB at detuning $\Delta = 0$.

To explore the statistic properties of the transmitted photons, the equal-time second-order correlation function $\log_{10}[g_{ij}^{(2)}(0)]$ ($ij = 12, 21$) is shown as a function of the detuning Δ/G in Fig. 2(c). The photon transport from port 2 to port 1 are coherent in full frequency, i.e., $g_{ij}^{(2)}(0) = 1$. The photons transport from port 1 to port 2 exhibit strong antibunching effect, i.e., $g_{ij}^{(2)}(0) \ll 1$, around the detunings $\Delta = \pm\sqrt{2}G$, and exhibit strong bunching effect, i.e., $g_{ij}^{(2)}(0) \gg 1$, around the detunings $\Delta = 0$ and $\pm 2G$. The time duration for nonreciprocal photon blockade at $\Delta = \pm\sqrt{2}G$ is on the order of $2\pi/(10\gamma_c)$, as shown in Fig. 2(d).

The peak for $T_{12} \approx 1$ at detuning $\Delta = 0$ can be understood by the fact that when the probe field is injected from port 2, only the (linear) optical mode a_L can be excited. Thus the maximum transmission coefficient is reached for the probe field in resonance with the optical mode a_L , i.e., $\Delta = 0$, and the transmitted photons keep the statistic properties of the probe field (a coherent field), i.e., $g_{12}^{(2)}(0) = 1$, for there is no nonlinear interactions in the optical path from port 2 to port 1.

In order to understand the origin of the peak for $T_{21} \approx 0.8$ around the detuning $\Delta = \pm\sqrt{2}G$ and the dip for $T_{21} \approx 10^{-7}$ at $\Delta = 0$, we use the ansatz that when the probe field input from port 1, the op-

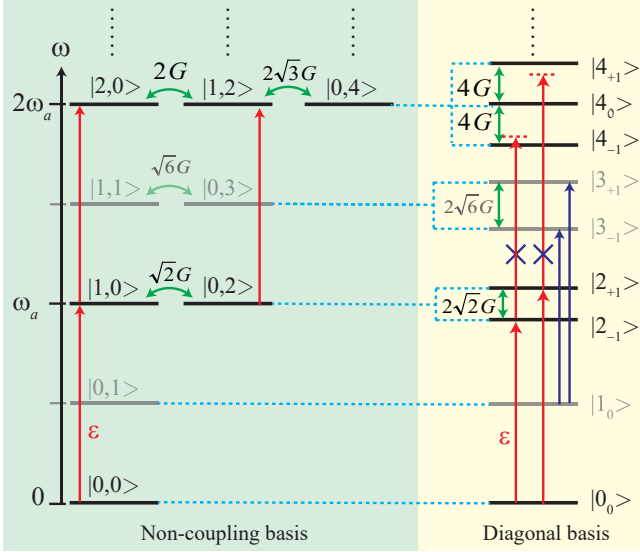


FIG. 3. (Color online) The schematic energy spectrum of the linearized quadratically optomechanical coupling between optical mode a_L and mechanical resonator b , given in the non-coupling basis (left) and in the diagonal basis (right).

tical mode a_L and the mechanical mode b will be excited, so the wave function can be written as $|\psi\rangle = C_{00}|0,0\rangle + C_{10}|1,0\rangle + C_{02}|0,2\rangle + \dots$, as shown in Fig. 3 (left). Here, $|n,m\rangle$ represents the Fock state with n photons in a_L and m phonons in b . The wave function can also be written in the diagonal basis as $|\psi\rangle = C_0|0_0\rangle + C_{1+}|2_{+1}\rangle + C_{1-}|2_{-1}\rangle + \dots$, as shown in Fig. 3 (right). Under weak probe condition, the maximum transmission coefficient $T_{21} \approx 0.8$ is reached for the probe field in resonance with the transition $|0_0\rangle \rightarrow |2_{\pm 1}\rangle$, i.e., $\Delta = \pm\sqrt{2}G$. However, the photons absorbed in the transition $|0_0\rangle \rightarrow |2_{\pm 1}\rangle$ blocks the transition $|2_{\pm 1}\rangle \rightarrow |4_{\pm 1}\rangle$ for large detuning, so we have $g_{12}^{(2)}(0) \ll 1$ around the detuning $\Delta = \pm\sqrt{2}G$. The dip for $T_{21} \approx 10^{-7}$ at $\Delta = 0$ arises from the quantum interference between the transitions $|2_{+1}\rangle \rightarrow |0_0\rangle$ and $|2_{-1}\rangle \rightarrow |0_0\rangle$, in an equivalent picture as optomechanically induced transparency [47–49], or electromagnetically induced transparency in lambda-type three-level atoms [50, 51]. Moreover, when $\Delta = 0$, the transition $|0_0\rangle \rightarrow |2_{\pm 1}\rangle$ is suppressed, but the two-photon transition $|0_0\rangle \rightarrow |4_0\rangle$ is resonant, which induces two-photon tunneling from port 1 to point 2, i.e., $g_{21}^{(2)}(0) \gg 1$. Similarly, $g_{21}^{(2)}(0) \gg 1$ around $\Delta = \pm 2G$ is induced by the resonant transition $|0_0\rangle \rightarrow |4_{\pm}\rangle$.

Before the end of this section, we discuss the effect of thermal phonons on the nonreciprocal photon blockade. Figures 4(a) and 4(c) show the transmission coefficient T_{21} and the equal-time second-order correlation function $\log_{10}[g_{21}^{(2)}(0)]$ versus the detuning Δ/G with different mean thermal phonon number ($n_{\text{th}} = 0, 0.1, 1$). Thermal phonons have little influence on the transmission coefficient T_{21} around $\Delta = \pm\sqrt{2}G$, but have great effect on the transmission coefficient T_{21} around $\Delta = 0$

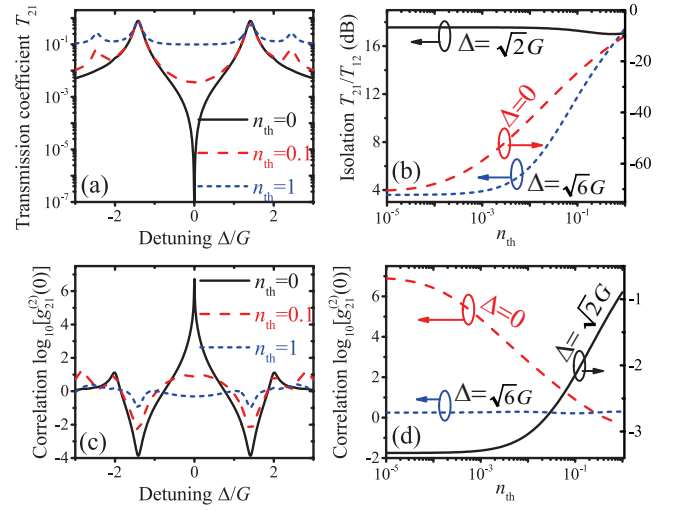


FIG. 4. (Color online) (a) The transmission coefficient T_{21} and (c) the equal-time second-order correlation function $\log_{10}[g_{21}^{(2)}(0)]$ versus the detuning Δ/G with different mean thermal phonon number ($n_{\text{th}} = 0, 0.1, 1$). (b) The isolation T_{21}/T_{12} and (d) the equal-time second-order correlation function $\log_{10}[g_{21}^{(2)}(0)]$ versus the mean thermal phonon number n_{th} with different detuning ($\Delta = 0, \sqrt{2}G, \sqrt{6}G$). The other parameters are the same as in Fig. 2.

and $\pm\sqrt{6}G$. Thermal phonons have little influence on the second-order correlation function $\log_{10}[g_{21}^{(2)}(0)]$ around $\Delta = \pm\sqrt{6}G$, but have great effect on the second-order correlation function $\log_{10}[g_{21}^{(2)}(0)]$ around $\Delta = 0$ and $\pm\sqrt{2}G$.

The relation of the isolation T_{21}/T_{12} and the second-order correlation function $\log_{10}[g_{21}^{(2)}(0)]$ on the mean thermal phonon number n_{th} are shown in Fig. 4(b) and 4(d) with detuning $\Delta = 0, \sqrt{2}G, \sqrt{6}G$. The isolation T_{21}/T_{12} around $\Delta = \sqrt{2}G$ is robust against the thermal phonons, but the antibunching effect of the transport photons become much weaker for greater thermal phonons. Both the isolation T_{21}/T_{12} and second-order correlation function $\log_{10}[g_{21}^{(2)}(0)]$ around $\Delta = 0$ are sensitive to the mean thermal phonon number n_{th} , and this quality may be used in accurate temperature measurement at ultra-low temperature. More interestingly, a peak appears around $\Delta = \pm\sqrt{6}G$ in the transmission coefficient T_{21} , and the isolation T_{21}/T_{12} can be improved with a larger thermal phonon number n_{th} . This abnormal effect is induced by the phonon states, e.g., $|1_0\rangle$ in Fig. 3(right). As the temperature increases, the population probability in $|1_0\rangle$ increases, and the transitions of $|1_0\rangle \rightarrow |3_{\pm 1}\rangle$ with resonance frequency $\Delta = \pm\sqrt{6}G$ become remarkable gradually, which induces the increasing peaks of the transmission coefficient T_{21} (or the isolation T_{21}/T_{12}) around $\Delta = \pm\sqrt{6}G$.

Finally, let us discuss the experimental feasibility of our proposal. In order to the photon correlation induced

by the weak probe field, we should spectrally filter out the strong optical driving field at $\Delta = \Delta_a$ under the condition $\Delta_a \gg \{\gamma_c, G\}$, which has already been realized in a recent experiment [52]. Another important condition required to observe nonreciprocal photon blockade in quadratically coupled optomechanical systems is the well-resolved sideband limit, i.e., $\omega_m \gg \gamma_c$. This requirement may be reached for a high frequency graphene sheet suspended on WGM microcavities [53] or photonic-crystal microcavities [54].

V. CONCLUSIONS

In summary, nonreciprocal photon blockade can be realized by directional nonlinear interactions. We have demonstrated this principle in an optomechanical system with quadratic optomechanical coupling. We explicitly show how quadratic optomechanical couplings between two WGM modes and one mechanical mode are generated when the linear optomechanical couplings vanishes in the normal optical modes. A quadratic optomechanical system with WGMs has been used to demonstrate nonreciprocal photon blockade. By optically pumping the WGM in one direction, the effective quadratic op-

tomechanical coupling is only enhanced in that direction, and consequently, the system exhibits nonreciprocal photon blockade. Moreover, the thermal phonons have important influence on the nonreciprocal photon blockade, especially on the statistic properties of the transport photons. Our proposal can have an application to unidirectional single-photon sources, unidirectional single-photon routers, single-photon isolators and circulators. This work can also be extended to study phonon manipulation in double-cavity optomechanics, e.g., nonreciprocal phonon blockade, nonreciprocal phonon laser [55–59], nonreciprocal photon-phonon entanglement and quantum transfer, etc.

Acknowledgement

We thank professor Yu-xi Liu for helpful discussions. X.W.X. is supported by the National Natural Science Foundation of China (NSFC) under Grants No.11604096 and the Startup Foundation for Doctors of East China Jiaotong University under Grant No. 26541059. Y.J.Z. is supported by the China Postdoctoral Science Foundation under grant No. 2017M620945. H.J. is supported by NSFC under Grant Nos. 11474087 and 11774086. A.X.C. is supported by NSFC under Grant No. 11775190.

-
- [1] D. Jalas, A. Petrov, M. Eich, W. Freude, S. Fan, Z. Yu, R. Baets, M. Popović, A. Melloni, J. D. Joannopoulos, M. Vanwolleghem, C. R. Doerr, and H. Renner, What is - and what is not - an optical isolator, *Nat. Photon.* **7**, 579 (2013).
- [2] R. Huang, A. Miranowicz, J. Q. Liao, F. Nori, H. Jing, Nonreciprocal Photon Blockade, arXiv:1807.10084 [quant-ph].
- [3] G. B. Malykin, The sagnac effect: correct and incorrect explanations, *Phys. Usp.* **43**, 1229 (2000).
- [4] H. Lü, Y. Jiang, Y. Z. Wang, and H. Jing, Optomechanically induced transparency in a spinning resonator, *Photonics Research* **5**, 000367 (2017).
- [5] S. Maayani, R. Dahan, Y. Kligerman, E. Moses, A. U. Hassan, H. Jing, F. Nori, D. N. Christodoulides, and T. Carmon, Flying couplers above spinning resonators generate irreversible refraction, *Nature (London)* **558**, 569 (2018).
- [6] D. W. Wang, H. T. Zhou, M. J. Guo, J. X. Zhang, J. Evers, and S. Y. Zhu, Optical Diode Made from a Moving Photonic Crystal, *Phys. Rev. Lett.* **110**, 093901 (2013).
- [7] S. A. R. Horsley, J. H. Wu, M. Artoni, and G. C. La Rocca, Optical Nonreciprocity of Cold Atom Bragg Mirrors in Motion, *Phys. Rev. Lett.* **110**, 223602 (2013).
- [8] H. Ramezani, P. K. Jha, Y. Wang, and X. Zhang, Nonreciprocal Localization of Photons, *Phys. Rev. Lett.* **120**, 043901 (2018).
- [9] T. J. Kippenberg and K. J. Vahala, Cavity Optomechanics: Back-Action at the Mesoscale, *Science* **321**, 1172 (2008).
- [10] F. Marquardt and S. M. Girvin, Optomechanics, *Physics* **2**, 40 (2009).
- [11] M. Aspelmeyer, P. Meystre, and K. Schwab, Quantum optomechanics, *Phys. Today* **65**(7), 29 (2012).
- [12] M. Aspelmeyer, T. J. Kippenberg, and F. Marquardt, Cavity Optomechanics, *Rev. Mod. Phys.* **86**, 1391 (2014).
- [13] M. Metcalfe, Applications of cavity optomechanics, *Appl. Phys. Rev.* **1**, 031105 (2014).
- [14] Y. L. Liu, C. Wang, J. Zhang, and Y. X. Liu, Cavity optomechanics: Manipulating photons and phonons towards the single-photon strong coupling, *Chin. Phys. B* **27**, 024204 (2018).
- [15] S. Manipatruni, J. T. Robinson, and M. Lipson, Optical Nonreciprocity in Optomechanical Structures, *Phys. Rev. Lett.* **102**, 213903 (2009).
- [16] M. Hafezi and P. Rabl, Optomechanically induced nonreciprocity in microring resonators, *Opt. Express* **20**, 7672 (2012).
- [17] M. Schmidt, S. Kessler, V. Peano, O. Painter, and F. Marquardt, Optomechanical creation of magnetic fields for photons on a lattice, *Optica* **2**, 635 (2015).
- [18] A. Metelmann and A. A. Clerk, Nonreciprocal Photon Transmission and Amplification via Reservoir Engineering, *Phys. Rev. X* **5**, 021025 (2015).
- [19] X. W. Xu and Y. Li, Optical nonreciprocity and optomechanical circulator in three-mode optomechanical systems, *Phys. Rev. A* **91**, 053854 (2015).
- [20] K. Fang, M. H. Matheny, X. Luan, and O. Painter, Optical transduction and routing of microwave phonons in cavity-optomechanical circuits, *Nat. Photon.* **10**, 489 (2016).
- [21] X. W. Xu, Y. Li, A. X. Chen, and Y. X. Liu, Nonreciprocal conversion between microwave and optical photons in electro-optomechanical systems, *Phys. Rev. A* **93**, 023827

- (2016).
- [22] A. Metelmann and A. A. Clerk, Non-reciprocal quantum interactions and devices via autonomous feed-forward, *Phys. Rev. A* **95**, 013837 (2017).
- [23] L. Tian and Z. Li, Nonreciprocal quantum-state conversion between microwave and optical photons, *Phys. Rev. A* **96**, 013808 (2017).
- [24] M.-A. Miri, F. Ruesink, E. Verhagen, and A. Alù, Optical Nonreciprocity Based on Optomechanical Coupling, *Phys. Rev. Applied* **7**, 064014 (2017).
- [25] G. Li, X. Xiao, Y. Li, and X. G. Wang, Tunable optical nonreciprocity and a phonon-photon router in an optomechanical system with coupled mechanical and optical modes, *Phys. Rev. A* **97**, 023801 (2018).
- [26] J. Kim, M. C. Kuzyk, K. Han, H. Wang, and G. Bahl, Non-reciprocal Brillouin scattering induced transparency, *Nat. Phys.* **11**, 275 (2015).
- [27] C. H. Dong, Z. Shen, C. L. Zou, Y. L. Zhang, W. Fu, and G. C. Guo, Brillouin-scattering-induced transparency and non-reciprocal light storage, *Nature Commun.* **6**, 6193 (2015).
- [28] Z. Shen, Y. L. Zhang, Y. Chen, C. L. Zou, Y. F. Xiao, X. B. Zou, F. W. Sun, G. C. Guo, and C. H. Dong, Experimental realization of optomechanically induced nonreciprocity, *Nature Photon.* **10**, 657 (2016).
- [29] F. Ruesink, M.-A. Miri, A. Alù, and E. Verhagen, Nonreciprocity and magnetic-free isolation based on optomechanical interactions. *Nat. Commun.* **7**, 13662 (2016).
- [30] K. Fang, J. Luo, A. Metelmann, M. H. Matheny, F. Marquardt, A. A. Clerk, O. Painter, Generalized nonreciprocity in an optomechanical circuit via synthetic magnetism and reservoir engineering, *Nat. Phys.* **13**, 465 (2017).
- [31] G. A. Peterson, F. Lecocq, K. Cicak, R. W. Simmonds, J. Aumentado, and J. D. Teufel, Demonstration of efficient nonreciprocity in a microwave optomechanical circuit, *Phys. Rev. X* **7**, 031001 (2017).
- [32] N. R. Bernier, L. D. Tóth, A. Kootandavida, A. Nunnenkamp, A. K. Feofanov, T. J. Kippenberg, Nonreciprocal reconfigurable microwave optomechanical circuit, *Nat. Commun.* **8**, 604 (2017).
- [33] S. Barzanjeh, M. Wulf, M. Peruzzo, M. Kalaei, P. B. Dieterle, O. Painter, and J. M. Fink, Mechanical On-Chip Microwave Circulator, *Nat. Commun.* **8**, 953 (2017).
- [34] H. Qiu, J. Dong, L. Liu, and X. Zhang, Energy-efficient on-chip optical diode based on the optomechanical effect, *Opt. Express* **25**, 8975 (2017).
- [35] Z. Shen, Y. L. Zhang, Y. Chen, F. W. Sun, X. B. Zou, G. C. Guo, C. L. Zou, and C. H. Dong, Reconfigurable optomechanical circulator and directional amplifier, *Nat. Commun.* **9**, 1797 (2018).
- [36] F. Ruesink, J. P. Mathew, M.-A. Miri, A. Alù, and E. Verhagen, Optical circulation in a multimode optomechanical resonator, *Nat. Commun.* **9**, 1798 (2018).
- [37] H. Xie, C. G. Liao, X. Shang, M. Y. Ye, and X. M. Lin, Phonon blockade in a quadratically coupled optomechanical system, *Phys. Rev. A* **96**, 013861 (2017).
- [38] G. Heinrich, J. G. E. Harris, and F. Marquardt, Photon shuttle: Landau-Zener-Stückelberg dynamics in an optomechanical system, *Phys. Rev. A* **81**, 011801(R) (2010).
- [39] H. Z. Wu, G. Heinrich, and F. Marquardt, The effect of Landau-Zener dynamics on phonon lasing, *New J. Phys.* **15**, 123022 (2013).
- [40] J. T. Hill, Nonlinear Optics and Wavelength Translation via Cavity-Optomechanics, Ph.D. thesis, California Institute of Technology, 2013.
- [41] T. K. Paraíso, M. Kalaei, L. Zang, H. Pfeifer, F. Marquardt, and O. Painter, Position-Squared Coupling in a Tunable Photonic Crystal Optomechanical Cavity, *Phys. Rev. X* **5**, 041024 (2015).
- [42] G. Anetsberger, O. Arcizet, Q. P. Unterreithmeier, R. Rivière, A. Schliesser, E. M. Weig, J. P. Kotthaus, and T. J. Kippenberg, Near-field cavity optomechanics with nanomechanical oscillators, *Nat. Phys.* **5**, 909 (2009).
- [43] C. Doolin, B. D. Hauer, P. H. Kim, A. J. R. MacDonald, H. Ramp, and J. P. Davis, Nonlinear optomechanics in the stationary regime, *Phys. Rev. A* **89**, 053838 (2014).
- [44] G. A. Brawley, M. R. Vanner, P. E. Larsen, S. Schmid, A. Boisen, and W. P. Bowen, Nonlinear optomechanical measurement of mechanical motion, *Nat. Commun.* **7**, 10988 (2016).
- [45] C. W. Gardiner and M. J. Collett, Input and output in damped quantum systems: Quantum stochastic differential equations and the master equation, *Phys. Rev. A* **31**, 3761 (1985).
- [46] H. J. Carmichael, An Open Systems Approach to Quantum Optics, Lecture Notes in Physics Vol. 18 (Springer-Verlag, Berlin, 1993).
- [47] G. S. Agarwal and S. Huang, Electromagnetically induced transparency in mechanical effects of light, *Phys. Rev. A* **81**, 041803(R) (2010).
- [48] S. Weis, R. Riviere, S. Deleglise, E. Gavartin, O. Arcizet, A. Schliesser, and T. J. Kippenberg, Optomechanically Induced Transparency, *Science* **330**, 1520 (2010).
- [49] A. H. Safavi-Naeini, T. P. Mayer Alegre, J. Chan, M. Eichenfield, M. Winger, Q. Lin, J. T. Hill, D. E. Chang, and O. Painter, Electromagnetically induced transparency and slow light with optomechanics, *Nature (London)* **472**, 69 (2011).
- [50] S. E. Harris, Electromagnetically Induced Transparency, *Phys. Today* **50**(7), 36 (1997).
- [51] M. Fleischhauer, A. Imamoglu, and J. P. Marangos, Electromagnetically induced transparency: Optics in coherent media, *Rev. Mod. Phys.* **77**, 633 (2005).
- [52] J. D. Cohen, S. M. Meenehan, G. S. MacCabe, S. Groblacher, A. H. Safavi-Naeini, F. Marsili, M. D. Shaw, and O. Painter, Phonon counting and intensity interferometry of a nanomechanical resonator, *Nature (London)* **520**, 522 (2015).
- [53] H. K. Li, Y. C. Liu, X. Yi, C. L. Zou, X. X. Ren, and Y. F. Xiao, Proposal for a near-field optomechanical system with enhanced linear and quadratic coupling, *Phys. Rev. A* **85**, 053832 (2012).
- [54] H. Wang, Q. Qiao, C. Peng, J. Xia, G. Zhou, Y. J. Zhao, and X. W. Xu, Two-dimensional optomechanics formed by the graphene sheet and photonic crystal cavity, arXiv:1806.00798 [quant-ph].
- [55] I. S. Grudin, H. Lee, O. Painter, and K. J. Vahala, Phonon Laser Action in a Tunable Two-Level System, *Phys. Rev. Lett.* **104**, 083901 (2010).
- [56] H. Wang, Z. Wang, J. Zhang, S. K. Özdemir, L. Yang, and Y. X. Liu, Phonon amplification in two coupled cavities containing one mechanical resonator, *Phys. Rev. A* **90**, 053814 (2014).
- [57] H. Lü, S. K. Özdemir, L. M. Kuang, F. Nori, and H. Jing, Exceptional Points in Random-Defect Phonon Lasers,

- Phys. Rev. Applied **8**, 044020 (2017).
- [58] Y. L. Zhang, C. L. Zou, C. S. Yang, H. Jing, C. H. Dong, G. C. Guo, and X. B. Zou, Phase-controlled phonon laser, New J. Phys. **20**, 093005 (2018).
- [59] J. Zhang, B. Peng, S. K. Özdemir, K. Pichler, D. O. Krimer, G. Zhao, F. Nori, Y. X. Liu, S. Rotter, and L. Yang, A phonon laser operating at an exceptional point, Nature Photon. **12**, 479 (2018).